



NIH Public Access

Author Manuscript

Biochemistry. Author manuscript; available in PMC 2013 July 17.

Published in final edited form as:

Biochemistry. 2012 July 17; 51(28): 5663–5673. doi:10.1021/bi300583s.

Structural organization of the nine spectrin repeats of Kalirin

KS Vishwanatha¹, YP Wang¹, HT Keutmann², RE Mains¹, and BA Eipper^{1,3,*}

¹Department of Neuroscience, University of Connecticut Health Center, Farmington, CT (06030), USA

²Endocrine Unit, Massachusetts General Hospital, Boston, MA 02115, USA

³Department of Molecular, Microbial and Structural Biology, University of Connecticut Health Center, Farmington, CT (06030), USA

Abstract

Sequence analysis suggests that *KALRN*, a Rho GDP/GTP exchange factor genetically linked to schizophrenia, could contain as many as nine tandem spectrin repeats (SRs). We expressed and purified fragments of Kalirin containing from one to five putative SRs in order to determine whether they formed nested structures that could endow Kalirin with the flexible rod-like properties characteristic of spectrin and dystrophin. Far UV circular dichroism studies indicated that Kalirin contains nine SRs. Based on thermal denaturation, sensitivity to chemical denaturants and the solubility of pairs of repeats, the nine SRs of Kalirin form nested structures. Modeling studies confirmed this conclusion and identified an exposed loop in SR5; consistent with the modeling, this loop was extremely labile to proteolytic cleavage. Analysis of a di-repeat fragment (SR4:5) encompassing the region of Kalirin known to interact with NOS2, DISC-1, PAM and Arf6 identified this as the least stable region. Analytical ultracentrifugation indicated that SR1:3, SR4:6 and SR7:9 were monomers and adopted an extended conformation. Gel filtration suggested that Δ Kal7, a natural isoform which includes SR5:9, was monomeric and was not more extended than SR5:9. Similarly, the nine SRs of Kal7, which was also monomeric, were not more extended than SR5:9. The rigidity and flexibility of the nine SRs of Kal7, which separate its essential N-terminal Sec14p domain from its catalytic domain, play an essential role in its contribution to the formation and function of dendritic spines.

Only four of over 60 Dbl family Rho GDP/GTP exchange factors (Rho-GEFs) encoded by the human genome include predicted spectrin repeats¹. The *KALRN*(*ARHGEF24*) and *TRIO*(*ARHGEF23*) genes each encode up to nine spectrin repeats while the *DBL* (*MCF2*; *ARHGEF21*) and *DBS* (*MCF2L*; *ARHGEF14*) genes include only one spectrin repeat. Neither the function nor the actual structure of these putative spectrin repeats has been examined. In all four proteins, the putative spectrin repeat region separates an N-terminal Sec14p-domain from the tandem DH-PH (Dbl Homology-Pleckstrin Homology) domain that catalyzes GDP/GTP exchange. The Sec14p domain of Kalirin binds specific phosphoinositides and is essential for function². Alternative splicing of the *KALRN* gene generates isoforms lacking the Sec14p and first four spectrin repeats, which cannot substitute for full-length isoforms. Kal7, the major full length isoform of Kalirin in adult brain, is localized at the post-synaptic density (PSD) in the dendritic spines receiving excitatory glutamatergic inputs (**Fig.1A**). The PH domain of Kal7 interacts with the juxtamembrane region of the NR2B subunit of the NMDA receptor³; with its catalytic domain near the plasma membrane, the nine spectrin repeats could position the lipid binding Sec14p domain of Kal7 outside of the PSD.

*Corresponding author (eipper@uchc.edu), phone: (860) 679-8898.

Each spectrin repeat consists of a left-handed, anti-parallel three-helix bundle 100 to 120 amino acids in length with aromatic residues at conserved sites; helices A, B and C are separated by non-helical linker regions referred to as the A/B and B/C loops^{4,5}. Erythroid and non-erythroid spectrin, with their multiple spectrin repeats and additional interaction domains, provide structural support to the plasma membrane by organizing an extensive cytoskeletal network and binding to multiple soluble and integral membrane proteins⁶. Dystrophin and utrophin, members of the spectrin superfamily, serve similar functions⁷. When expressed in non-neuronal cells, Kal7 also localizes to the subplasma membrane cytoskeleton⁸. Based on crystallographic analysis of fragments of spectrin, α -actinin, utrophin and dystrophin, the C-helix of one repeat is connected to the A-helix of the next repeat by a helical linker, forming a functional unit^{7,9-12}. The junction between two spectrin repeats forms the ankyrin binding site in β 1-spectrin and is sensitive to alterations in orientation^{5,13,14}. The putative spectrin repeat region of Kal7 interacts with peptidylglycine α -amidating monooxygenase (PAM), NOS2, DISC-1, HAP1, Arf6, sorting nexins 1 and 2, and α II-spectrin¹⁵⁻¹⁹. The NOS2 interaction site is the junction between spectrin repeats 4 and 5 (SR4 and SR5) of Kalirin²⁰.

To determine whether the region separating the Sec14p and first GEF domains of Kalirin actually consists of nine spectrin repeats and to manipulate the interaction of Kalirin with its targets, we expressed and purified fragments comprising one to five spectrin repeats. Stable proteins were purified and analyzed using circular dichroism, gel filtration, ultracentrifugation and molecular modeling. The properties of Δ Kal7 and Kal7 were compared to those of the smaller fragments.

Materials and Methods

Design and subcloning of recombinant spectrin repeat proteins

The numbering scheme for rat Kalirin produced from the α -promoter is used throughout (rat Kalirin-9a: AAF66018.1; GI:7650388). The boundaries of each predicted spectrin repeat were initially defined using the SMART database, which recognizes only 7 of the 9 domains referred to as SRs by Alam et al.¹⁵ (<http://smart.embl-heidelberg.de>); the SR terminology used by Alam et al. is utilized, although neither the region between SR5 and SR7 nor the region between SR7 and SR9 is predicted by SMART to adopt the conformation of a spectrin repeat. To ensure proper folding, we extended the N- and C-termini of the tandem spectrin repeat constructs by a few residues. The start and stop sites for each protein are given in **Table 1**; the name of each protein indicates the spectrin repeat regions it includes (e.g. SR4:7 contains spectrin repeats 4 through 7). cDNAs encoding most of the spectrin repeat fragments were subcloned into the pGEX-6P-2 vector using an upstream BamHI restriction site and a downstream NotI site. All vectors were verified by sequencing. A Prescission Protease site separates GST from the spectrin repeat region in the pGEX-6P-2 constructs while a thrombin site is present in pGEX-4T-2, which was used to produce KalSR4:6.

Preparation of recombinant SR proteins

The cDNAs encoding each fusion protein were transformed into *Escherichia coli* BL21. To facilitate folding of the recombinant fusion protein, growth and induction [0.4mM isopropyl- β -D thiogalactopyranoside (Sigma-Aldrich, St. Louis, MO) for 2h] were carried out at 20°C; this increased the yield of soluble product significantly. Yields for each spectrin repeat protein ranged from 0.5-5mg/500 ml bacterial culture. The cell pellet from a 500ml culture was washed twice with PBS (50mM NaPi, 150mM NaCl, pH 7.4), resuspended in 30ml PBS and lysed using a Misonix S4000 ultrasonic liquid processor (Qsonica, LLC, Newtown, CT). Insoluble debris was removed by centrifugation (3 \times 14,000rpm for 30min) and the filtered

supernatant was loaded onto a 5ml GSTrap-4B column (GE Healthcare, Piscataway, NJ) equilibrated with PBS (flow rate 0.5ml/min). After equilibration with cleavage buffer (25mM Tris-HCl, pH 8.0, 150mM NaCl, 14mM β -mercaptoethanol), each SR protein was cleaved from glutathione S-transferase using GST-HRVC3 protease (GenWay Biotech, Inc., San Diego, CA) (10 Units/mg fusion protein); the cartridge was incubated with protease overnight at 4°C. The GST moiety was removed from KalSR4:6 using thrombin (Sigma Aldrich, St. Louis, MO). Each SR protein was subjected to anion exchange chromatography on a Q-Sepharose column equilibrated with 20mM NaTES, pH 7.0 and eluted with a gradient to 0.5 M NaCl (60ml over 120min) in the same buffer. The purity and homogeneity of each SR protein was evaluated by SDS-PAGE (BioRad Criterion TGXTM gels, 4 to 15% gradient) followed by staining with Coomassie Brilliant Blue R250. The concentration of each SR protein was determined by measuring its absorbance at 280 nm and using the extinction coefficient calculated from its content of tryptophan and tyrosine (**Table 1**).

Circular Dichroism and Thermal Unfolding

Far UV-CD spectra were recorded using a Jasco J-715 spectropolarimeter equipped with a thermostated cell housing, using a cell with a 1-mm path length. SR proteins (6 μ M) were examined between 190 and 260nm. Molar ellipticity per mean residue, Θ in deg cm² dmol⁻¹ was calculated from the equation: $[\Theta] = [\Theta]_{\text{obs}} \cdot M_{\text{rw}} / 10Ic$, where $[\Theta]_{\text{obs}}$ is the ellipticity measured in degrees, M_{rw} is the mean residue molecular weight (110g mol⁻¹), c is the protein concentration in g L⁻¹ and I is the optical path length of the cell in cm. The scan speed was 10nm/min at a bandwidth of 1nm. An average of three runs were recorded for each protein sample. Secondary structure analysis of each SR protein was carried out using CDSSTR²¹ with the reference database available in DICHROWEB (<http://dichroweb.cryst.bbk.ac.uk/html/home.shtml>).

For determination of the thermal unfolding profile, the temperature was increased from 20-90°C at a rate of 1°C/min and the ellipticity from 190-260nm was recorded at 5°C intervals. To test for reversibility, all the samples were cooled back to 20°C and the CD spectra were again recorded. Thermal unfolding transitions and midpoints (T_m) were obtained by plotting normalized ellipticity values at 222nm as a function of temperature.

Unfolding by chemical denaturants

Stock solutions of 6 M guanidine hydrochloride and 8M urea (Sigma-Aldrich, St. Louis, MO) were prepared in 20mM NaTES, pH 7.0. Concentrations of denaturants were determined by measuring the refractive indices. In each chemical denaturation experiment, recombinant SR protein (final concentration 2 μ M) was incubated for 12h with either 0 to 4M GuHCl or 0 to 6M urea at 27°C in the dark. Unfolding was initiated by addition of a concentrated protein stock to the appropriate denaturant. Unfolding curves were obtained by plotting normalized ellipticity values at 222nm as a function of denaturant concentration.

Molecular modeling

For the generation of three dimensional models of tandem spectrin repeats, we used the automated I-TASSER server (<http://zhanglab.ccmn.med.umich.edu/I-TASSER/>). Models were displayed and analyzed in PyMOL (Delano Scientific). To define individual helices along with their connecting loops and to assign individual residues to *a* and *d* positions in the heptad hydrophobic repeats, we first aligned the nine spectrin repeat sequences using CLUSTALW (<http://www.genome.jp/tools/clustalw/>). The boundaries of the helices and connecting loops were then assigned based on the three dimensional models generated.

Sedimentation velocity analysis

Sedimentation velocity experiments were carried out at 20°C (55,000rpm) in 20mM NaTES, 200mM NaCl, pH 7.0 buffer using either interference optics in a Beckman-Coulter XL-I (Brea, CA) analytical ultracentrifuge or fluorescence optics in an XL-I analytical ultracentrifuge equipped with an AU-FDS detector (AVIV). Double sector cells equipped with quartz windows were used. The rotor was equilibrated under vacuum at 20°C and after a period of ~1h the rotor was accelerated to 55,000rpm. Absorbance scans at 280nm were acquired at ~4.5 minute intervals for 7h. Protein molecular weights (MW_{seq}), partial specific volumes (ν_{20°), extinction coefficients (ϵ_{230nm}) and buffer density and viscosity were calculated using SEDNTERP²². Sedimentation velocity data were analyzed with the time-derivative of concentration profile method using the program DcDt+ to obtain weight-average sedimentation coefficient distribution [$g(s)$] values²³; continuous sedimentation coefficient [$c(s)$] distribution plots were obtained by SEDPHAT²³. SEDPHAT analysis yields direct values for the Stokes radius (R_s) and frictional coefficient (f/f_{min}).

Determination of Stokes radius by gel permeation chromatography

The Stokes radius was determined using gel filtration chromatography on a Superose 6 10/300 GL column equilibrated with 200mM NaCl, 20mM NaTES, pH 7.0. The proteins used for calibration and their Stokes radii were: apo ferritin (6.3nm), human IgG (5.52nm), bovine serum albumin dimer (4.3nm), bovine serum albumin monomer (3.55nm), ovalbumin (2.73nm) and cytochrome *c* (1.77nm)²⁴. The protein peaks were monitored using a UV detector. For analysis of HisMycKal7 and HisMycΔKal7, pEAK Rapid cells transiently transfected with the appropriate expression vector² were lysed in 20mM NaTES, 10mM mannitol, pH 7.4; particulate material was removed by centrifugation at 14,000 × g for 15min and aliquots of the supernatant were loaded onto the Superose 6 column in the presence of thyroglobulin (1mg) and bovine serum albumin (1mg). Aliquots of each fraction were subjected to SDS-PAGE; elution position was determined after staining with Coomassie Brilliant Blue or Western blot analysis using an antibody specific for the C-terminus of Kal7. The void volume (V_0) was determined using high molecular weight blue dextran. The elution volumes (V_e) of individual standard proteins and SR proteins were recorded. A calibration curve was obtained by plotting the Stokes radius of each standard as a function of elution volume. Since the SRs are elongated, rod like molecules based on sedimentation analysis, Stokes radii for SR5:9, HisMycKal7 and HisMycΔKal7 were obtained from a calibration curve generated using the R_s values for SRs that were determined by analytical ultracentrifugation. The f/f_{min} values for SR5:9, HisMycKal7 and HisMycΔKal7 were obtained by using the deduced R_s value in Stokes and Perrin equations²⁵.

Results

Analysis of recombinant Kalirin SR proteins using circular dichroism

Fourteen Kalirin SR proteins containing between one and five putative SRs were expressed as GST fusion proteins (Fig. 1 and Table 1). All were expressed at high levels, but six of the fusion proteins were largely insoluble and one (SR9) had a very low degree of solubility. The purity of the seven soluble Kalirin SR proteins examined in this study is shown in Fig. 1C. The concentration of each purified SR protein was determined using the extinction coefficient calculated from its sequence (Table 1).

The secondary structure of the tri-repeat SR1:3 protein was determined by far UV circular dichroism (CD) spectroscopy (Fig. 2A). The intense negative peaks at 208nm and 222nm are typical of proteins with a substantial amount of α -helical structure²⁶; analysis with CDSSTR indicates that 58% of the residues in SR1:3 are α -helical (Table 2). The ratio

between the minima at 222nm and 208nm was 1.05 for SR1:3, indicating that the helices present in this structure interact with each other²⁷. The stability of SR1:3 was assessed by determining its resistance to heat-induced denaturation, which was monitored by CD spectra recorded at 222nm. Thermal unfolding of SR1:3 could be resolved into two phases (**Fig. 2B**); a steep unfolding curve with a midpoint of 41°C occurred first, followed by a second transition with a midpoint of 64°C. Native molar ellipticity was not regained upon cooling the sample to 20°C, indicating that the unfolding process was irreversible.

Most of the interactions of Kalirin with other proteins involve spectrin repeats 4 through 6, making the structure of this region of special interest. In addition, the isoforms of Kalirin lack SR1 through SR4, placing SR5 at the N-terminus. For these reasons, pairs of spectrin repeats were examined (SR4:5, SR5:6) along with the tri-repeat SR4:6 protein that would be present in full-length Kalirin but absent from the ΔKalirin isoforms (**Fig. 1A**). Far UV CD spectra for SR4:5, SR5:6 and SR4:6 were typical of proteins rich in α-helical structure (**Fig. 3A**). As observed for SR1:3, the $\Theta_{222}/\Theta_{208}$ ratios for all three proteins were greater than 1.00 (**Table 2**). The thermal melting profiles for all three proteins indicated cooperative unfolding with a single T_m . SR4:5 had the lowest thermal stability; a single cooperative transition with a midpoint of 32°C was observed, suggesting the presence of a poorly ordered domain at physiological temperature (**Fig. 3B**). Although the thermal unfolding profile for SR4:5 shows “gain of structure” at higher temperatures, the far UV CD spectra recorded between 190 and 260 nm revealed the presence of unstructured random coils. SR5:6 and SR4:6 were more stable than SR4:5; these proteins each had a T_m of 42°C and each unfolded as a single unit (**Fig. 3B** and **Table 1**). The addition of SR6 to SR4:5 resulted in increased thermal stability, suggesting conformational coupling between spectrin repeats in the central region of Kalirin.

The far UV CD spectrum of the final tri-repeat protein, SR7:9, again revealed a protein with a significant amount of α-helix (49%) and interacting helices (**Fig. 4A** and **Table 2**). SR7:9 showed a single thermal transition with a midpoint of 46°C (**Fig. 4B**). In order to explore the existence of conformational stabilization from adjacent spectrin repeats, we examined two longer SR proteins, SR4:7 and SR5:9. The Far UV CD spectra for both proteins were indicative of structures rich in α-helix with interacting helices (**Fig. 4A** and **Table 2**). Thermal denaturation of both proteins was bi-phasic (**Fig. 4B**). Like SR4:5, the structure of SR4:7 was unstable at physiological temperature; T_m values of 31°C and 46°C were observed. SR5:9, the entire spectrin repeat region present in the Δ isoforms of Kalirin, exhibited T_m values of 42°C and 62°C (**Fig. 4B**); neither SR5:6 nor SR7:9 had a T_m value as high as that observed in the larger protein.

Chemically induced unfolding of Kalirin SR proteins

To further explore the properties of the spectrin repeat regions critical to the interactions of Kalirin with other proteins, we assessed the ability of SR4:5, SR5:6, SR4:6 and SR4:7 to resist denaturation by guanidine HCl (0 to 4 M) or urea (0 to 6 M). Each SR protein was exposed to denaturant for 12 h and circular dichroism at 222 nm was then assessed (**Fig. 5** and **Table 3**). When exposed to either guanidine HCl or urea, SR4:5 unfolded cooperatively, indicating a two-state process (**Fig. 5**); SR4:5 unfolded at a lower concentration of each denaturant than the other SR proteins examined. Complete unfolding of SR5:6 required higher concentrations of both guanidine HCl and urea, with unfolding in guanidine HCl occurring in two stages. The tri-repeat SR4:6 and tetra-repeat SR4:7 proteins unfolded in two distinctly different stages, suggestive of regions that unfold independently; both of these larger proteins contained denaturant resistant regions. Based on both its lack of thermal stability and sensitivity to chemical denaturants, SR4:5 is less stable than the surrounding spectrin repeats.

Molecular modeling of spectrin repeat region

The biophysical properties of the fragments of Kalirin examined are consistent with the presence of nine spectrin repeats in Kal7. Molecular modeling of each tri-repeat protein, SR1:3, SR4:6 and SR7:9, was also consistent with this hypothesis (**Fig. 6A**). When analyzed as part of SR4:6 or SR4:5, the B/C loop of SR5 was predicted to contain a short region of α -helix (**Fig. 6B**). We subjected GST-SR4:7 to limited trypsin digestion in order to determine whether this putative helical region was accessible, as predicted by modeling (**Fig. 6C**). Cleavage products #1, #2 and #3 were subjected to Edman degradation. The first trypsin cleavage separated GST from SR4:7. Sequence data could not be obtained for product #2, suggesting the presence of N-terminal heterogeneity. Product #3, a stable proteolytic product, was generated by cleavage after Arg⁷⁰⁴, which is located in the short helical region predicted to occur in the B/C loop of SR5.

The sequences of the nine spectrin repeats of Kalirin were aligned based on these structural predictions (**Fig. 7**). The amino acids included in the A, B and C helices and in the A/B and B/C connecting loops were assigned based on the models shown. The amino acids of each heptad repeat are identified as *a* to *g*, with *a* and *d* constituting the hydrophobic core of the coiled-coils. The region following the N-terminal Sec14p domain of Kalirin was assigned to SR1; this 142 amino acid region is longer than the typical spectrin repeat. Modeling predicts a long loop preceding helix A of SR1, leaving a short A/B loop connecting helix A to helix B. Seven of the nine SR proteins have tryptophan at the 14th position of helix A. The B helix of each spectrin repeat is substantially longer than the A- or C-helix. The A/B loop of SR8 is substantially longer than other A/B loop and includes a short helical region. The B/C loops of SR1, SR3, SR5 and SR6 range in length from 17 to 21 residues while the B/C loops of the remaining SRs are much shorter (2 to 5 residues). A binding motif for SH3 domains appears in the B/C loop of SR3 and a helical region is included in the B/C loop of SR5.

Hydrodynamic properties of SR proteins

Sedimentation velocity analysis was used to determine whether the SR proteins adopted the extended structures predicted by molecular modeling and to determine whether they formed oligomers. Each SR protein was examined at three different concentrations. Analysis of SR1:3, SR4:6 and SR7:9 revealed a single component whose sedimentation velocity was independent of concentration (**Fig. 8**). The evaluation of $S_{20,w}$ from the experimental s-value was accomplished by fitting the data to Sedphat²³. Data for each of the SR proteins examined are summarized in **Table 4A** [apparent molecular weight ($M_{w,app}$), $S_{20,w}$ and Stokes radius]. The molecular weight of each SR protein measured by sedimentation velocity is very close to the value calculated from the sequence, indicating that each SR protein behaved as a monomer in solution. Reversible self association was not observed, even at the highest concentration examined (**Fig. 8**); a small amount of aggregated material was present. The experimentally determined Stokes radii indicate that each SR protein adopts an extended rod-like structure, with frictional ratios for the tri-repeat proteins varying from 1.46 for SR7:9 to 1.60 for SR1:3.

In order to compare the properties of the recombinant SR proteins to those of Kal7 and Δ Kal7, we utilized gel permeation chromatography. A calibrated Superose 6 column was used to analyze each recombinant protein (**Fig. 9A**). The gel filtration standards analyzed are globular²⁵, and a plot of their elution volume vs. their Stokes radius generated the expected straight line. Since the SR proteins are rod-shaped, a plot of their elution volumes vs. their experimentally determined Stokes radius generated a line shifted to the left (**Fig. 9A**). Gel filtration analysis of purified SR5:9 and cell lysates containing Δ Kal7 or Kal7 allowed us to estimate their Stokes radii based on the standard curve generated using purified SR proteins (**Fig. 9B** and **Table 4B**). Glycerol gradient analysis of Δ Kal7 and Kal7 from cell lysates

eliminated the possibility that either of these proteins dimerized. The Stokes radius was then used to calculate a frictional ratio (f/f_{min}) for each monomeric protein; SR5:9, with five spectrin repeats, has a frictional ratio greater than that of SR4:7, which has four spectrin repeats. Despite their substantially greater molecular weights, neither Δ Kal7 nor Kal7 exhibits greater asymmetry than SR5:9. Kal7, with nine spectrin repeats, has a frictional ratio less than that of Δ Kal7.

Discussion

Kalirin contains nine spectrin-like repeats

Although more variable in length than the SRs of spectrin and dystrophin, our analyses indicate that Kalirin contains nine spectrin repeats. Each SR is about ~5 nm long, meaning that a single molecule of Kal7 could extend over 45 nm, a significant distance within the typical 300 nm diameter and 40 nm thick post-synaptic density²⁸. Based on circular dichroism, the α -helical content of the Kalirin SRs varied from 42% to 58%; the α -helical content of the 24 spectrin repeats of dystrophin is higher, ranging from 55% to 100%²⁹. Conservation of inward facing non-polar residues in heptad repeats allows the helices to interact with each other. Our circular dichroism data, with the ratio between the minima at 222 nm and 208 nm >1.0 for each Kalirin SR fragment examined, indicate that the helices interact²⁷. Thermal denaturation revealed cooperative unfolding of each Kalirin SR fragment, with T_m values between 32 and 64°C. Di-repeat fragments of spectrin exhibited T_m values that varied over the same range (36 to 63°C)⁹. The low thermal stability of selected spectrin repeats suggests a role in making the larger protein flexible or in forming a binding site for interacting proteins. While thermal denaturation of individual spectrin repeats is generally reversible, that of tandem repeats is not³⁰. None of the Kalirin proteins examined adopted their native conformation after thermal denaturation. The cooperative unfolding of fragments of Kalirin and spectrin required similar concentrations of urea⁹.

Adjacent spectrin repeats form functional units

When tandem spectrin repeats are connected by a helical linker that joins the C-helix of the first unit to the A-helix of the second unit, an elongated, non-globular structure is formed and the folding of one spectrin repeat is linked to the folding of neighboring repeats^{9,29,30}. SR3 of Kalirin could be stably expressed as part of SR1:3, but not as SR3:6 or SR3:7. SR1:3 exhibits two distinct thermal unfolding transitions, suggesting the presence of regions that fold independently. If the presence of SR2 stabilizes SR3, perhaps by joining the C-helix of SR2 to the short A-helix of SR3, SR1 may fold separately. Based on analysis of SR4:5, SR5:6, SR4:6 and SR4:7, SR4 is more sensitive to thermal and chemical denaturation than other regions. While SR4:6 exhibits a single thermal unfolding transition, its response to urea and guanidine demonstrates the presence of independent domains. The response of SR5:6 to thermal denaturation and urea suggests the presence of a single unit, leading to the suggestion that SR4 folds separately. Thermal denaturation of SR7:9 occurs with a single transition, indicative of the presence of nested spectrin repeats. The biphasic thermal denaturation of SR5:9 is consistent with the presence of two domains, one formed by SR5:6 and the other by SR7:9. Non-coincidence of thermal and chemical denaturation curves was observed for fragments of human erythroid spectrin⁹, as for SR5:6 and SR4:6; it is difficult to predict which denaturant will reveal the presence of multiple units.

Like SR4:5 of Kalirin, selected repeats in spectrin and dystrophin are largely unfolded at physiological temperature^{9,10}. Only the full-length isoforms of Kalirin contain SR4; the Δ -isoforms begin with SR5. The fact that SR4:5 is unfolded at physiological temperatures may provide the conformational flexibility needed for Kalirin to form a docking station for other proteins. The ability of Kalirin to interact with NOS2 was mapped to the 30 amino acid

peptide that includes helix C of SR4 and helix A of SR5^{16,20}. The binding of PAM¹⁵, HAP-1³¹, DISC-1³² and Arf6¹⁷ to Kalirin has not been as finely mapped, but includes this same region. The junction between SR4 and SR5 would be surrounded by the A/B loop of SR4 and the B/C loop of SR5; based on its sensitivity to trypsin, the 13 amino acid α -helical region contained in the B/C loop of SR5 is accessible (**Fig. 6C**). Both desmoplakin³³ and plakin³⁴ contain spectrin repeats in which a B/C loop contains an additional folded region. Src homology 3 (SH3) domains inserted into the SRs of plakin³⁴, desmoplakin³³ and α -spectrin³⁵ interact with other proteins. The SH3 binding motif in the B/C loop of SR3 has been shown to interact with the SH3 motif present in the larger isoforms of Kalirin³⁶ and the helical folds in the B/C loops of SR5 and SR8 may be engaged in protein-protein interactions.

Selected spectrin repeat regions of erythroid and neuronal spectrin^{37,38} and dystrophin^{39,40} interact with plasma membrane lipids. Preliminary studies suggest that the spectrin repeat regions of Kalirin bind to liposomes; further study will be required to identify the SRs involved and to determine the role of these interactions. As for spectrin and dystrophin, the ability of the spectrin repeat regions of Kalirin to interact with membrane lipids would be expected to play an essential role in its effects on the secretory and endocytic pathways.

High resolution structures of spectrin repeats from α -and β -spectrin^{11,41-43}, α -actinin^{44,45}, utrophin^{7,46} and dystrophin^{7,12,47} reveal curved helices that wrap around each other. Variability resides in the length and conformation of the A-B and B-C loops and the linkers connecting adjacent repeats. With α -helical linkers connecting adjacent units, the angle between adjacent units can vary substantially. Ankyrin binds tightly to the junction between spectrin repeats 14 and 15 of β -spectrin; since SR15 is tilted compared to SR14, binding is thought to be sensitive to mechanical deformation⁵.

Kalirin is an elongated monomer

The α - and β -chains of spectrin form heterodimers which join in head-to-head tetramers; the helical content and thermal stability of monomeric α - and β -spectrin are similar to those of native spectrin⁴⁸. While α -actinin homodimerizes^{47,49,50}, dystrophin is a monomer²⁹. Based on sedimentation velocity, each of the Kalirin SR fragments examined is monomeric; while some amount of aggregation was observed, they showed no tendency to form oligomers.

The frictional coefficient, f , depends on the size and shape of the molecule. The f/f_{min} ratio provides a good indication of whether a protein is globular or elongated²⁵. Nested SRs form elongated, non-globular structures⁴⁵ and the f/f_{min} ratios observed for the di-, tri-, and tetra-SR proteins examined (**Table 4**) indicate that each adopts this type of structure^{49,51-53}. SR4:5 and SR5:6 have f/f_{min} ratios of 1.37 and 1.47, respectively. Of the three tri-repeat SR proteins examined, SR1:3 has the highest ratio (1.60). The ratio for SR4:7 (1.65) is higher than for SR4:6 (1.47).

For SR5:9, Δ Kal7 and Kal7, f/f_{min} ratios were estimated using a gel filtration column calibrated with the proteins analyzed in the ultracentrifuge; SR5:9 ($f/f_{min}=1.75$) appears to be even more extended than SR4:7. The f/f_{min} value for Δ Kal7 (1.71) is not increased over that of SR5:9, indicating that the GEF domain, which crystallographic studies identify as a compact 10nm × 10 nm × 9.8 nm structure⁵⁴, does not form a rigid extension of SR5:9. The fact that Thr¹⁵⁹⁰, a Cdk5 phosphorylation site located immediately beyond the GEF domain, is readily accessible in constructs that lack any spectrin repeats but is not readily accessible in Δ Kal7, is consistent with an intramolecular interaction between the spectrin repeat and C-terminal regions of Δ Kal7⁵⁵. Although Kal7 differs from Δ Kal7 by the addition of SR1:4 and Sec14p, the f/f_{min} value for Kal7 (1.63) is smaller than that of Δ Kal7. Given the

instability of SR4, it is tempting to suggest that its presence introduces flexibility into Kal7, allowing its N-terminal region to interact with the rest of the molecule.

Acknowledgments

We thank Darlene D'Amato for her contributions to all aspects of this work, Li Luo for her assistance with circular dichroism and Mathilde Bonnemaison for her suggestions on how to present the data. We also thank Dr. Jeffery Lary, Analytical Ultracentrifugation facility, UConn, Storrs for his help with ultracentrifugation study.

Funding

This work was supported by NIH grant DK-32948 to REM and by the Janice and Rodney Reynolds Endowment.

Abbreviations

SR	spectrin repeat
PSD	post-synaptic density
PAM	Peptidylglycine α -Amidating Monooxygenase
GST	glutathione S-transferase
CD	circular dichroism

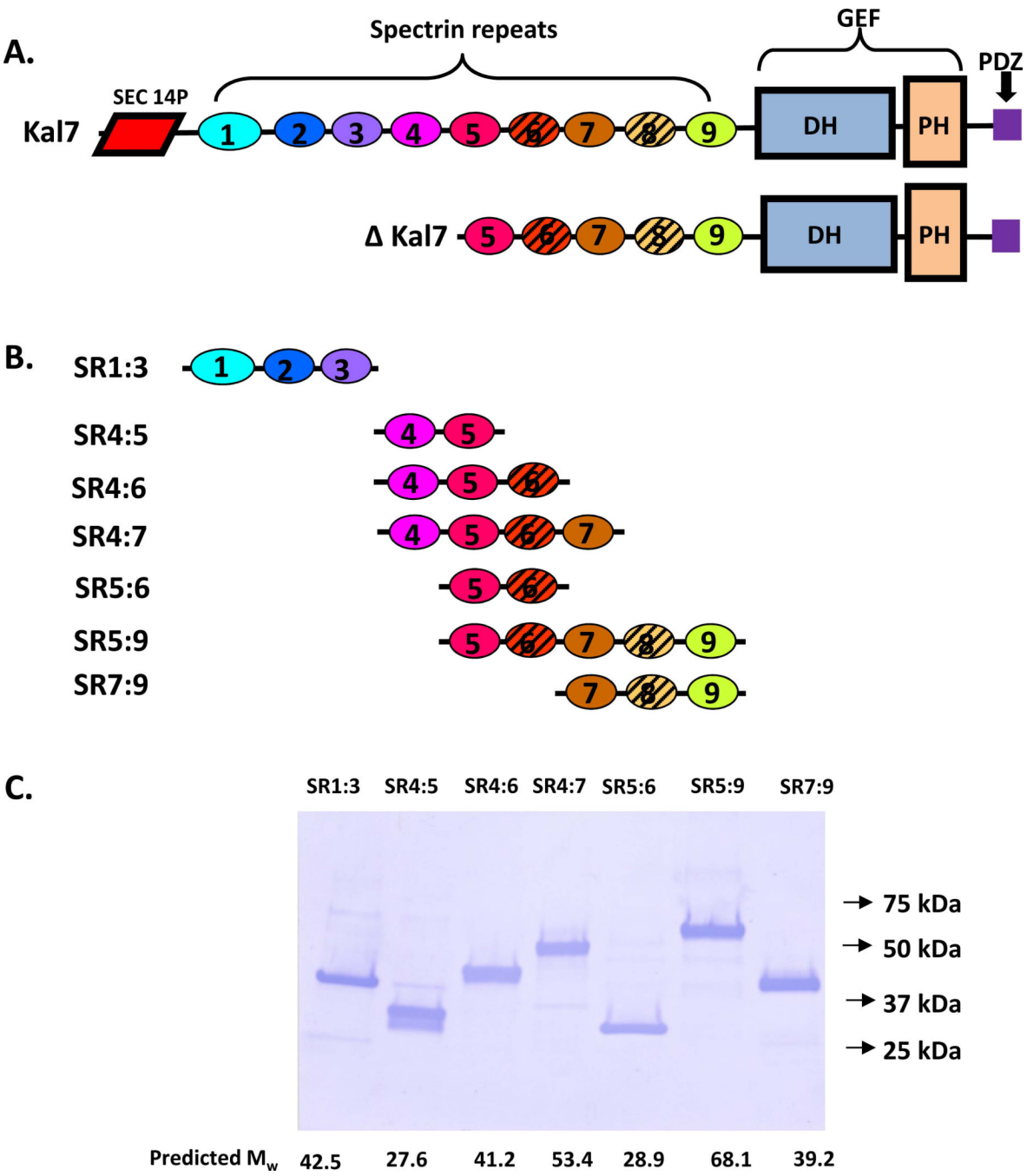
References

1. Rossman KL, Sondek J. Larger than Dbl: new structural insights into RhoA activation. *Trends Biochem. Sci.* 2005; 30:163–165. [PubMed: 15817389]
2. Schiller MR, Blangy A, Huang J, Mains RE, Eipper BA. Induction of lamellipodia by Kalirin does not require its guanine nucleotide exchange factor activity. *Exp. Cell Res.* 2005; 307:402–417. [PubMed: 15950621]
3. Kiraly DD, Lemtiri-Chlieh F, Levine ES, Mains RE, Eipper BA. Kalirin binds the NR2B subunit of the NMDA receptor, altering its synaptic localization and function. *J. Neurosci.* 2011; 31:12554–12565. [PubMed: 21880917]
4. Speicher DW, Marchesi VT. Erythrocyte spectrin is comprised of many homologous triple helical segments. *Nature.* 1984; 311:177–180. [PubMed: 6472478]
5. Stabach PR, Simonovic I, Ranieri MA, Aboodi MS, Steitz TA, Simonovic M, Morrow JS. The structure of the ankyrin-binding site of beta-spectrin reveals how tandem spectrin-repeats generate unique ligand-binding properties. *Blood.* 2009; 113:5377–5384. [PubMed: 19168783]
6. Lombardo CR, Weed SA, Kennedy SP, Forget BG, Morrow JS. Beta II-spectrin (fodrin) and beta I epsilon 2 spectrin (muscle) contain NH2- and COOH-terminal membrane association domains (MAD1 and MAD2). *J. Biol. Chem.* 1994; 269:29212–29219. [PubMed: 7961888]
7. Winder SJ, Gibson TJ, Kendrick-Jones J. Dystrophin and utrophin: the missing links! *FEBS Lett.* 1995; 369:27–33. [PubMed: 7641878]
8. Schiller MR, Ferraro F, Wang Y, Ma XM, McPherson CE, Sobota JA, Schiller NI, Mains RE, Eipper BA. Autonomous functions for the Sec14p/spectrin-repeat region of Kalirin. *Exp. Cell Res.* 2008; 314:2674–2691. [PubMed: 18585704]
9. MacDonald RI, Cummings JA. Stabilities of folding of clustered, two-repeat fragments of spectrin reveal a potential hinge in the human erythroid spectrin tetramer. *Proc. Natl. Acad. Sci. U. S. A.* 2004; 101:1502–1507. [PubMed: 14747656]
10. Kusunoki H, MacDonald RI, Mondragon A. Structural insights into the stability and flexibility of unusual erythroid spectrin repeats. *Structure.* 2004; 12:645–656. [PubMed: 15062087]
11. Pascual J, Pfuhl M, Walther D, Saraste M, Nilges M. Solution structure of the spectrin repeat: a left-handed antiparallel triple-helical coiled-coil. *J. Mol. Biol.* 1997; 273:740–751. [PubMed: 9356261]

12. Norwood FL, Sutherland-Smith AJ, Keep NH, Kendrick-Jones J. The structure of the N-terminal actin-binding domain of human dystrophin and how mutations in this domain may cause Duchenne or Becker muscular dystrophy. *Structure*. 2000; 8:481–491. [PubMed: 10801490]
13. Davis L, Abdi K, Machius M, Brautigam C, Tomchick DR, Bennett V, Michaely P. Localization and structure of the ankyrin-binding site on beta2-spectrin. *J. Biol. Chem.* 2009; 284:6982–6987. [PubMed: 19098307]
14. Ipsaro JJ, Huang L, Mondragon A. Structures of the spectrin-ankyrin interaction binding domains. *Blood*. 2009; 113:5385–5393. [PubMed: 19141864]
15. Alam MR, Johnson RC, Darlington DN, Hand TA, Mains RE, Eipper BA. Kalirin, a cytosolic protein with spectrin-like and GDP/GTP exchange factor-like domains that interacts with peptidylglycine alpha-amidating monooxygenase, an integral membrane peptide-processing enzyme. *J. Biol. Chem.* 1997; 272:12667–12675. [PubMed: 9139723]
16. Ratovitski EA, Alam MR, Quick RA, McMillan A, Bao C, Kozlovsky C, Hand TA, Johnson RC, Mains RE, Eipper BA, Lowenstein CJ. Kalirin inhibition of inducible nitric-oxide synthase. *J. Biol. Chem.* 1999; 274:993–999. [PubMed: 9873042]
17. Koo TH, Eipper BA, Donaldson JG. Arf6 recruits the Rac GEF Kalirin to the plasma membrane facilitating Rac activation. *BMC. Cell Biol.* 2007; 8:29. [PubMed: 17640372]
18. Rabiner CA, Mains RE, Eipper BA. Kalirin: a dual Rho guanine nucleotide exchange factor that is so much more than the sum of its many parts. *Neuroscientist*. 2005; 11:148–160. [PubMed: 15746383]
19. Prosser DC, Tran D, Schooley A, Wendland B, Ngsee JK. A novel, retromer-independent role for sorting nexins 1 and 2 in RhoG-dependent membrane remodeling. *Traffic*. 2010; 11:1347–1362. [PubMed: 20604901]
20. Youn H, Ji I, Ji HP, Markesberry WR, Ji TH. Under-expression of Kalirin-7 Increases iNOS activity in cultured cells and correlates to elevated iNOS activity in Alzheimer's disease hippocampus. *J. Alzheimers. Dis.* 2007; 12:271–281. [PubMed: 18057561]
21. Sreerama N, Woody RW. Structural composition of betaI- and betaII-proteins. *Protein Sci.* 2003; 12:384–388. [PubMed: 12538903]
22. Laue, TM.; Shah, BD.; Ridgeway, TM.; Pelletier, SL. Computer-aided interpretation of analytical sedimentation data for proteins; in Analytical Ultracentrifugation in Biochemistry and Polymer Science. In: Harding, S.; Rowe, A., editors. Royal Society of Chemistry; 1992. p. 90-125.
23. Schuck P. On the analysis of protein self-association by sedimentation velocity analytical ultracentrifugation. *Anal. Biochem.* 2003; 320:104–124. [PubMed: 12895474]
24. Le Maire M, Arnou B, Olesen C, Georgin D, Ebel C, Moller JV. Gel chromatography and analytical ultracentrifugation to determine the extent of detergent binding and aggregation, and Stokes radius of membrane proteins using sarcoplasmic reticulum Ca²⁺-ATPase as an example. *Nat. Protoc.* 2008; 3:1782–1795. [PubMed: 18974737]
25. Erickson HP. Size and shape of protein molecules at the nanometer level determined by sedimentation, gel filtration, and electron microscopy. *Biol. Proced. Online*. 2009; 11:32–51. [PubMed: 19495910]
26. Sreerama N, Venyaminov SY, Woody RW. Estimation of the number of alpha-helical and beta-strand segments in proteins using circular dichroism spectroscopy. *Protein Sci.* 1999; 8:370–380. [PubMed: 10048330]
27. Zhang YP, Lewis RN, Hodges RS, McElhaney RN. FTIR spectroscopic studies of the conformation and amide hydrogen exchange of a peptide model of the hydrophobic transmembrane alpha-helices of membrane proteins. *Biochemistry*. 1992; 31:11572–11578. [PubMed: 1445892]
28. Chen X, Winters C, Azzam R, Li X, Galbraith JA, Leapman RD, Reese TS. Organization of the core structure of the postsynaptic density. *Proc. Natl. Acad. Sci. U. S. A.* 2008; 105:4453–4458. [PubMed: 18326622]
29. Mirza A, Sagatelian M, Sahni N, Choi L, Menhart N. A biophysical map of the dystrophin rod. *Biochim. Biophys. Acta*. 2010; 1804:1796–1809. [PubMed: 20382276]

30. An X, Zhang X, Salomao M, Guo X, Yang Y, Wu Y, Gratzer W, Baines AJ, Mohandas N. Thermal stabilities of brain spectrin and the constituent repeats of subunits. *Biochemistry*. 2006; 45:13670–13676. [PubMed: 17087521]
31. Colomer V, Engelender S, Sharp AH, Duan K, Cooper JK, Lanahan A, Lyford G, Worley P, Ross CA. Huntingtin-associated protein 1 (HAP1) binds to a Trio-like polypeptide, with a rac1 guanine nucleotide exchange factor domain. *Hum. Mol. Genet.* 1997; 6:1519–1525. [PubMed: 9285789]
32. Hayashi-Takagi A, Takaki M, Graziene N, Seshadri S, Murdoch H, Dunlop AJ, Makino Y, Seshadri AJ, Ishizuka K, Srivastava DP, Xie Z, Baraban JM, Houslay MD, Tomoda T, Brandon NJ, Kamiya A, Yan Z, Penzes P, Sawa A. Disrupted-in-Schizophrenia 1 (DISC1) regulates spines of the glutamate synapse via Rac1. *Nat. Neurosci.* 2010; 13:327–332. [PubMed: 20139976]
33. Choi HJ, Weis WI. Crystal structure of a rigid four-spectrin-repeat fragment of the human desmoplakin plakin domain. *J. Mol. Biol.* 2011; 409:800–812. [PubMed: 21536047]
34. Ortega E, Buey RM, Sonnenberg A, de Pereda JM. The structure of the plakin domain of plectin reveals a non-canonical SH3 domain interacting with its fourth spectrin repeat. *J. Biol. Chem.* 2011; 286:12429–12438. [PubMed: 21288893]
35. Bialkowska K, Saido TC, Fox JE. SH3 domain of spectrin participates in the activation of Rac in specialized calpain-induced integrin signaling complexes. *J. Cell Sci.* 2005; 118:381–395. [PubMed: 15632109]
36. Schiller MR, Chakrabarti K, King GF, Schiller NI, Eipper BA, Maciejewski MW. Regulation of RhoGEF activity by intramolecular and intermolecular SH3 domain interactions. *J. Biol. Chem.* 2006; 281:18774–18786. [PubMed: 16644733]
37. An X, Guo X, Gratzer W, Mohandas N. Phospholipid binding by proteins of the spectrin family: a comparative study. *Biochem. Biophys. Res. Commun.* 2005; 327:794–800. [PubMed: 15649416]
38. Ray S, Chakrabarti A. Membrane interaction of erythroid spectrin: surface-density-dependent high-affinity binding to phosphatidylethanolamine. *Mol. Membr. Biol.* 2004; 21:93–100. [PubMed: 15204438]
39. Sarkis J, Hubert JF, Legrand B, Robert E, Cheron A, Jardin J, Hitti E, Le Rumeur E, Vie V. Spectrin-like repeats 11–15 of human dystrophin show adaptations to a lipidic environment. *J. Biol. Chem.* 2011; 286:30481–30491. [PubMed: 21712383]
40. Legardinier S, Raguenes-Nicol C, Tascon C, Rocher C, Hardy S, Hubert JF, Le Rumeur E. Mapping of the lipid-binding and stability properties of the central rod domain of human dystrophin. *J. Mol. Biol.* 2009; 389:546–558. [PubMed: 19379759]
41. Yan Y, Winograd E, Viel A, Cronin T, Harrison SC, Branton D. Crystal structure of the repetitive segments of spectrin. *Science*. 1993; 262:2027–2030. [PubMed: 8266097]
42. Grum VL, Li D, MacDonald RI, Mondragon A. Structures of two repeats of spectrin suggest models of flexibility. *Cell*. 1999; 98:523–535. [PubMed: 10481916]
43. Kusunoki H, Minasov G, MacDonald RI, Mondragon A. Independent movement, dimerization and stability of tandem repeats of chicken brain alpha-spectrin. *J. Mol. Biol.* 2004; 344:495–511. [PubMed: 15522301]
44. Tang J, Taylor DW, Taylor KA. The three dimensional structure of alpha-actinin obtained by cryoelectron microscopy suggests a model for Ca(2+)-dependent actin binding. *J. Mol. Biol.* 2001; 310:845–858. [PubMed: 11453692]
45. Djinovic-Carugo K, Gautel M, Ylanne J, Young P. The spectrin repeat: a structural platform for cytoskeletal protein assemblies. *FEBS Lett.* 2002; 513:119–123. [PubMed: 11911890]
46. Keep NH, Winder SJ, Moores CA, Walke S, Norwood FL, Kendrick-Jones J. Crystal structure of the actin-binding region of utrophin reveals a head-to-tail dimer. *Structure*. 1999; 7:1539–1546. [PubMed: 10647184]
47. Kahana E, Gratzer WB. Minimum folding unit of dystrophin rod domain. *Biochemistry*. 1995; 34:8110–8114. [PubMed: 7794924]
48. Fujita T, Ralston GB, Morris MB. Purification of erythrocyte spectrin alpha- and beta-subunits at alkaline pH and structural and hydrodynamic properties of the isolated subunits. *Biochemistry*. 1998; 37:272–280. [PubMed: 9425048]
49. Flood G, Rowe AJ, Critchley DR, Gratzer WB. Further analysis of the role of spectrin repeat motifs in alpha-actinin dimer formation. *Eur. Biophys. J.* 1997; 25:431–435. [PubMed: 9188165]

50. Flood G, Kahana E, Gilmore AP, Rowe AJ, Gratzer WB, Critchley DR. Association of structural repeats in the alpha-actinin rod domain. Alignment of inter-subunit interactions. *J. Mol. Biol.* 1995; 252:227–234. [PubMed: 7674303]
51. Ralston GB. Physical-chemical studies of spectrin. *J. Supramol. Struct.* 1978; 8:361–373. [PubMed: 723271]
52. Long F, McElheny D, Jiang S, Park S, Caffrey MS, Fung LW. Conformational change of erythroid alpha-spectrin at the tetramerization site upon binding beta-spectrin. *Protein Sci.* 2007; 16:2519–2530. [PubMed: 17905835]
53. Rybakova IN, Humston JL, Sonnemann KJ, Ervasti JM. Dystrophin and utrophin bind actin through distinct modes of contact. *J. Biol. Chem.* 2006; 281:9996–10001. [PubMed: 16478721]
54. Skowronek KR, Guo F, Zheng Y, Nassar N. The C-terminal basic tail of RhoG assists the guanine nucleotide exchange factor trio in binding to phospholipids. *J. Biol. Chem.* 2004; 279:37895–37907. [PubMed: 15199069]
55. Xin X, Wang Y, Ma XM, Rompolas P, Keutmann HT, Mains RE, Eipper BA. Regulation of Kalirin by Cdk5. *J. Cell Sci.* 2008; 121:2601–2611. [PubMed: 18628310]

**Fig. 1. Kalirin proteins examined**

A. The domain structures predicted for Kal7 and Δ Kal7, a naturally occurring splice variant, are shown; SR6 and SR8, which are not recognized as spectrin-like repeats by SMART, are stippled. The catalytic Dbl homology (DH) and adjacent pleckstrin homology (PH) domain form the GDP/GTP exchange factor domain. The C-terminus of Kal7 is a Type 1 PDZ binding motif, Ser-Thr-Tyr-Val. **B.** The SR proteins indicated were expressed as GST fusion proteins, cleaved and purified. **C.** The seven purified SR proteins studied (1 μ g of each) were subjected to SDS-PAGE, transferred to a PVDF membrane and visualized using Coomassie Brilliant Blue 250. The mass of the molecular weight markers is indicated, as is the molecular weight (M_w) predicted for each SR protein.

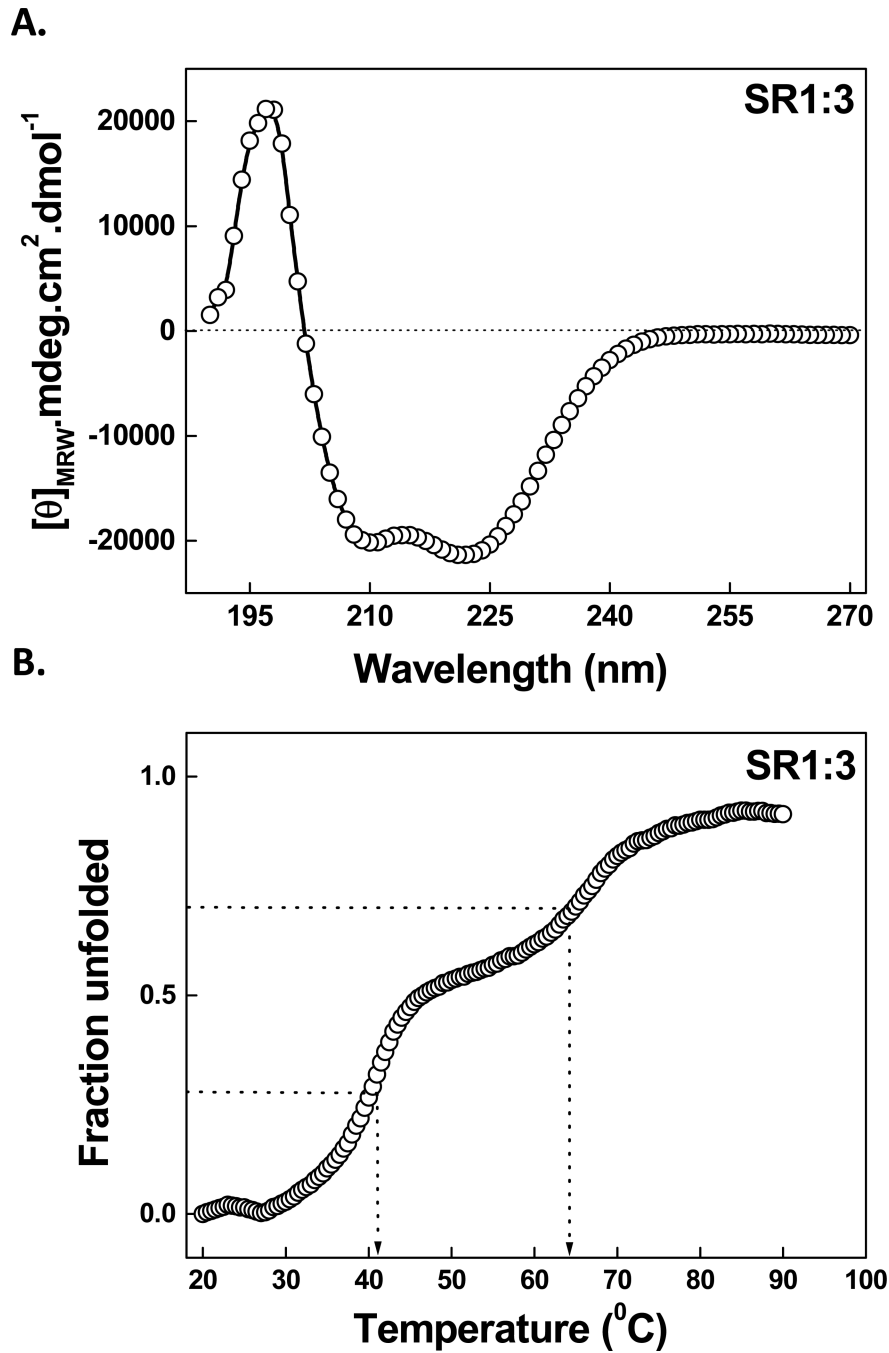
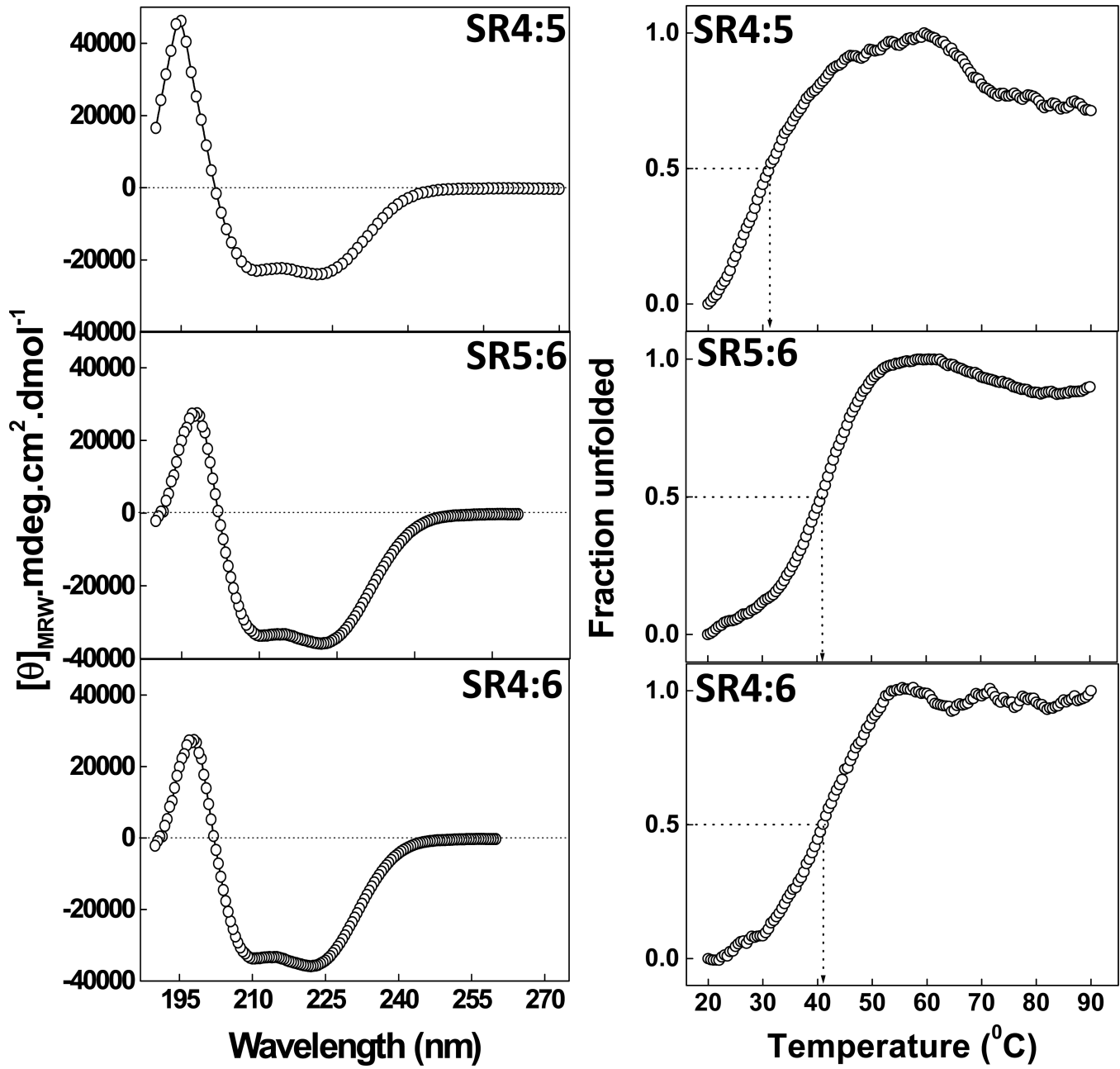


Fig. 2. Circular dichroism – SR1:3

A. The far UV CD spectrum for SR1:3 is shown. **B.** The fraction of SR1:3 that was unfolded during a thermal denaturation experiment monitored at 222nm is shown. Data from multiple analyses of SR1:3 are summarized in **Table 2**.

**Fig. 3. Circular dichroism – SR4:5, SR5:6 and SR4:6**

The far UV CD spectra for SR4:5, SR5:6 and SR4:6 and the fraction of each protein that was unfolded during a thermal denaturation experiment monitored at 222 nm are shown. Data from multiple analyses of SR4:5, SR5:6 and SR4:6 are summarized in **Table 2**.

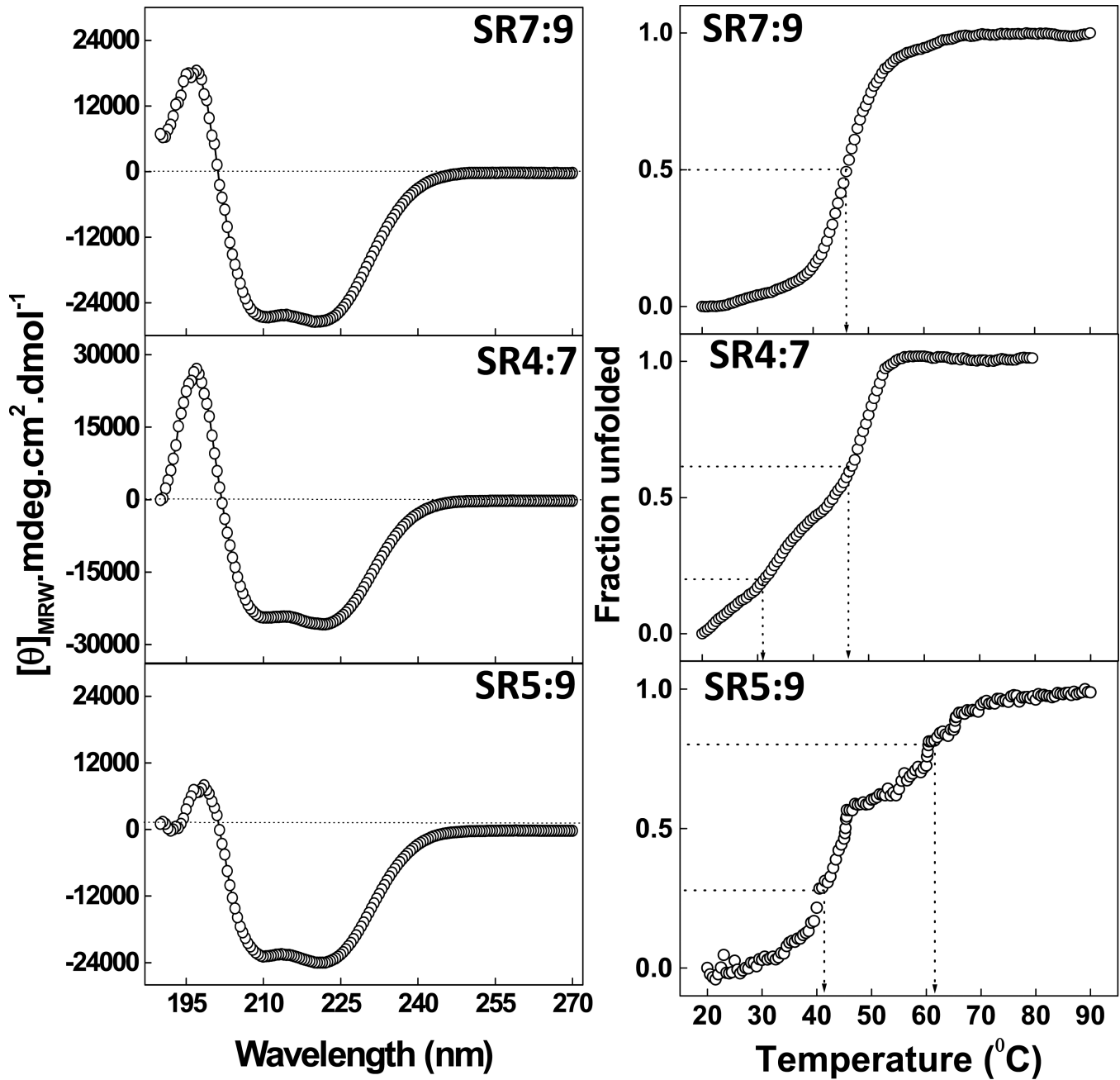


Fig. 4. Circular dichroism – SR4:7, SR7:9 and SR5:9

The far UV CD spectra for SR4:7, SR7:9 and SR5:9 and the fraction of each protein that was unfolded during a thermal denaturation experiment monitored at 222 nm are shown. Data from multiple analyses of SR4:7, SR7:9 and SR5:9 are summarized in **Table 2**.

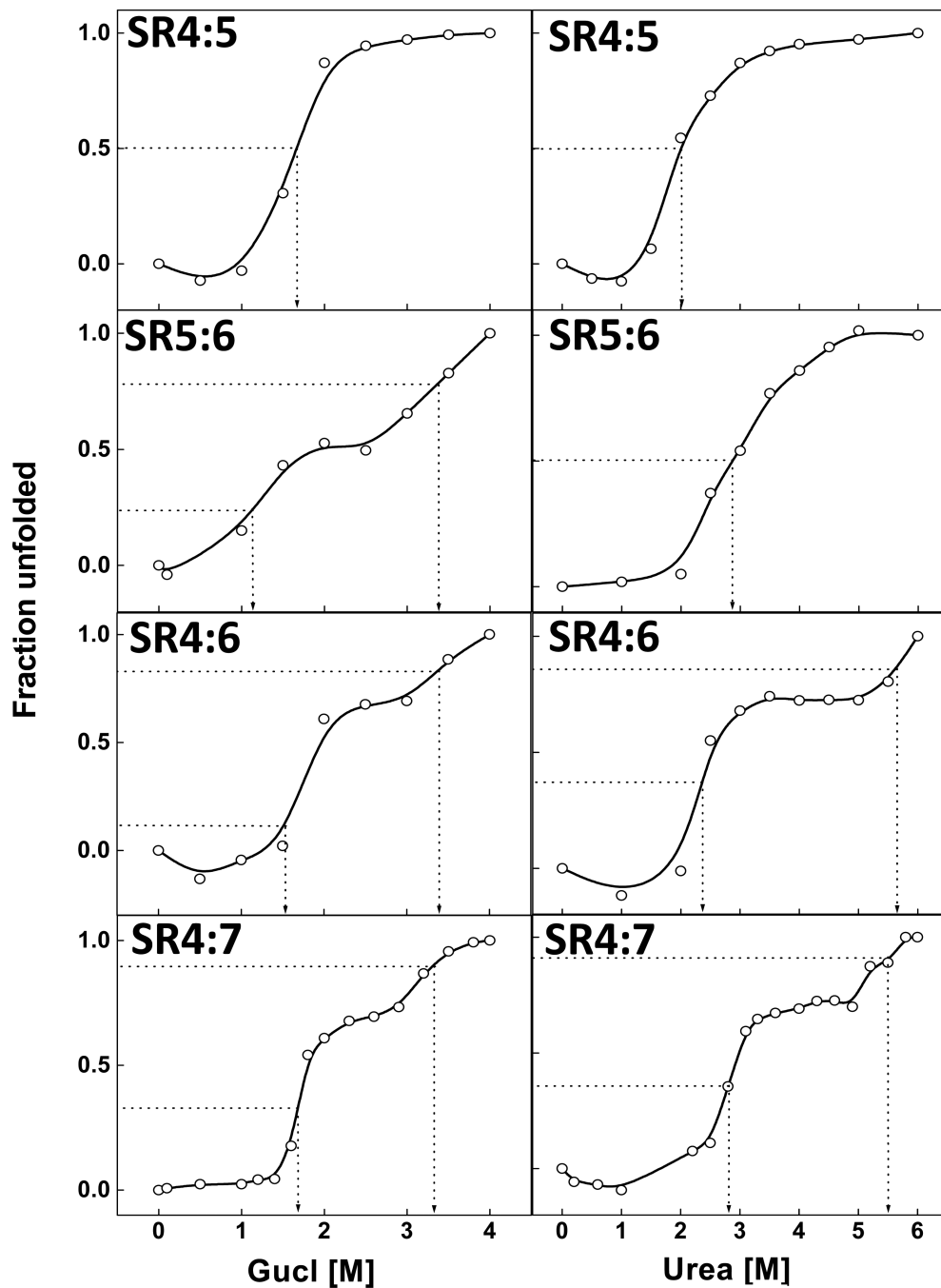
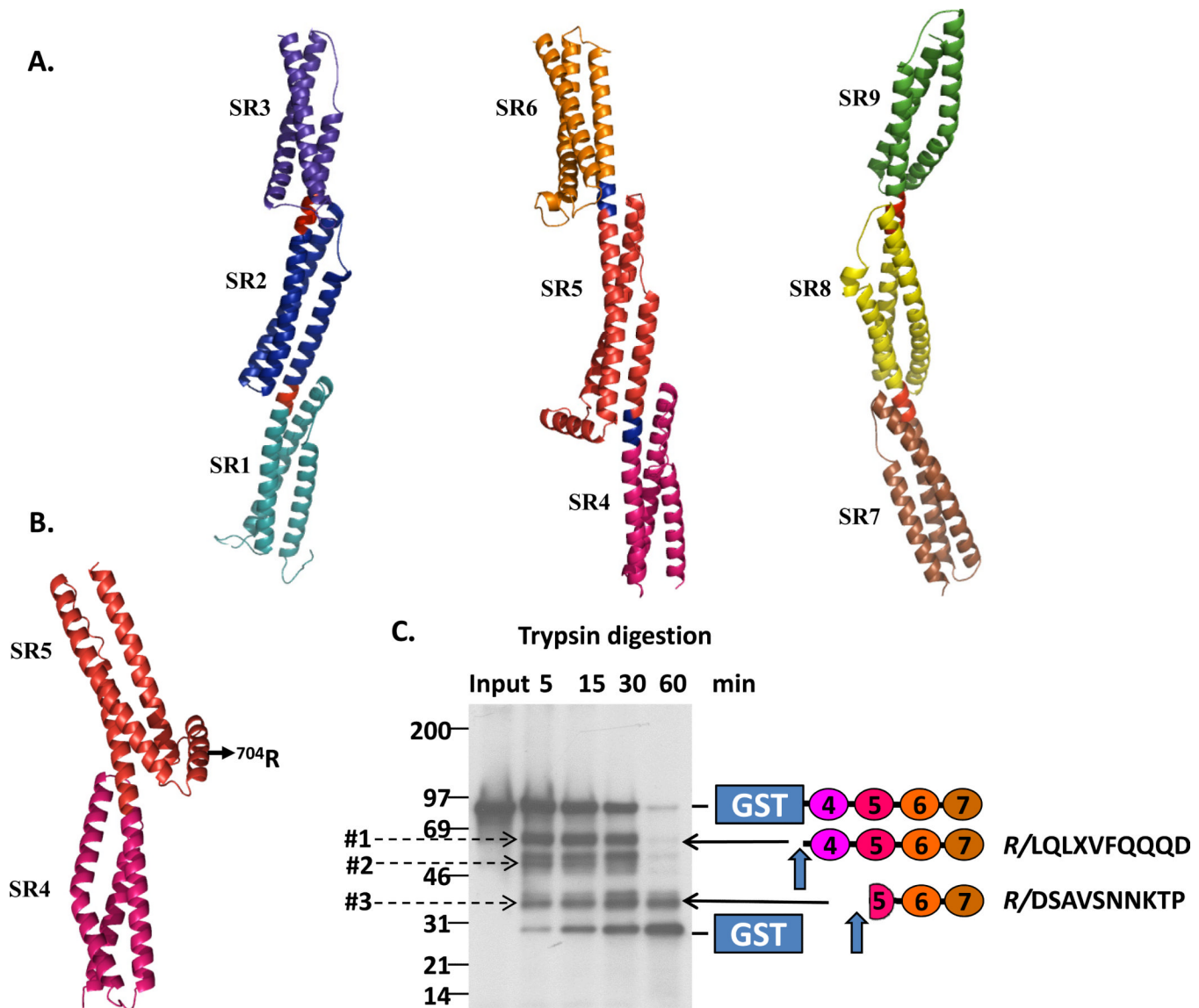


Fig. 5. Sensitivity to chemical denaturants

SR4:5, SR5:6, SR4:6 and SR4:7 were incubated in guanidine HCl (0 to 4.0 M) or urea (0 to 6.0 M) for 12h at 27°C and then subjected to far UV CD analysis. The fraction of each protein unfolded was assessed by monitoring the signal at 222 nm. Data for the different SR proteins are summarized in **Table 3**.

**Fig. 6. Results of molecular modeling**

A. The sequences of the three tri-repeat SR proteins were submitted to the automated I-TASSER server (<http://zhanglab.ccmb.med.umich.edu/I-TASSER/>). Each SR is indicated by a different color; the linker regions connecting adjacent repeats are shown in red (SR1:3 and SR7:9) or blue (SR4:6). **B.** The backbone structures predicted for the di-repeat SR4:5 protein are shown in an orientation that highlights the helical region in the B/C linker. **C.** Purified GST-SR4:7 was incubated with immobilized TPCK trypsin (Pierce) for the times indicated, fractionated by SDS-PAGE and visualized using antisera to SR4:7. Only the top and bottom bands were visualized using antibody to GST; the antisera used was not affinity-purified and recognizes both SR4:7 and GST. A larger amount of GST-SR4:7 was treated with immobilized trypsin for 30 min and fractionated by SDS-PAGE. The Coomassie stained bands (#1, #2, #3) indicated by black arrows were excised from the PVDF membrane and subjected to Edman degradation using an Applied Biosystems Model 477A pulsed-liquid sequencer with on-line HPLC identification; the cleavage sites (blue arrows) and sequences obtained are shown.

NIH-PA Author Manuscript

NIH-PA Author Manuscript

NIH-PA Author Manuscript

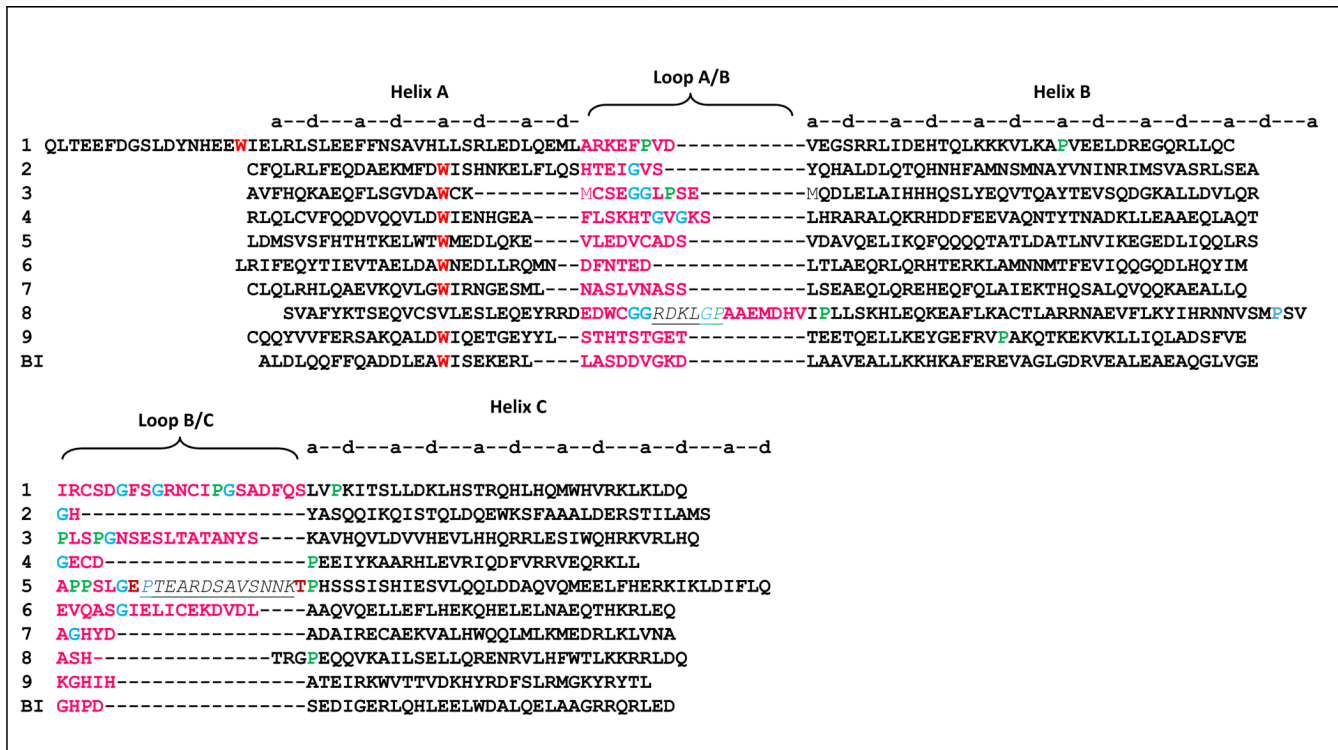


Fig. 7. Revised identification of helix and loop regions in the spectrin repeat region of Kalirin
The A, B and C helices of the nine spectrin repeats of Kalirin identified by molecular modeling are indicated. Pro residues are depicted in green. Helical regions predicted within the A/B and B/C loops are shown in underlined *Italics*. The sequence of SR1 of human erythroid β I spectrin⁵ is shown for comparison.

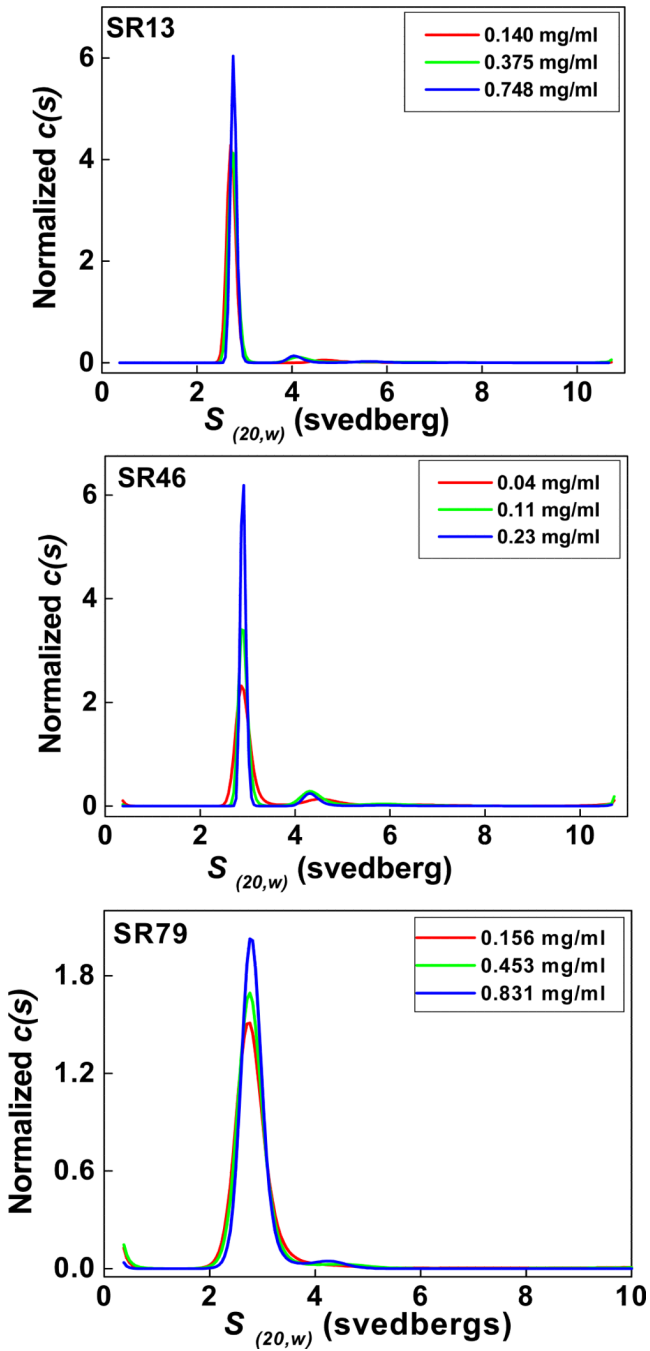
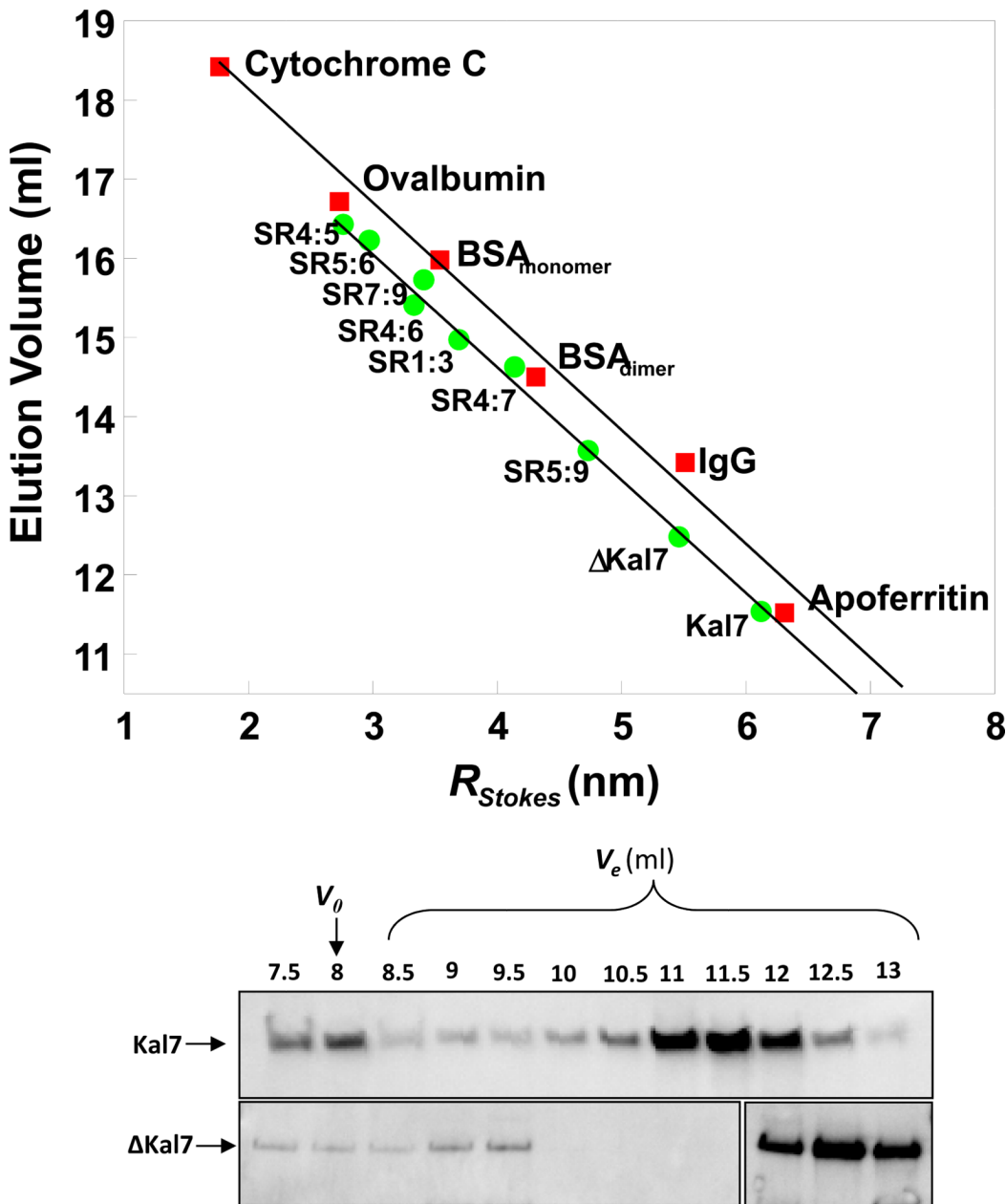


Fig. 8. Analytical ultracentrifugation

SR1:3, SR4:5, SR5:6, SR4:6, SR4:7 and SR7:9 were subjected to analytical ultracentrifugation. Data for three concentrations of SR1:3, SR4:6 and SR7:9 are shown; there was no indication of reversible dimerization. The calculated mass for each SR protein analyzed indicates that it is monomeric. The frictional ratios determined (**Table 4**) indicate that each of these proteins is an extended rod.

**Fig. 9. Gel filtration**

SR proteins were analyzed on a Superose 6 column calibrated using the indicated globular protein standards. The elution volume for each globular protein is plotted against its published Stokes radius (red squares)²⁵. The elution volume for each SR protein subjected to analytical ultracentrifugation is plotted against its experimentally determined Stokes radius (green circles). Purified SR5:9 and lysates of non-neuronal cells transiently expressing Kal7 or ΔKal7 were analyzed on the same column; their elution volumes were determined by Western blot analysis of individual fractions. Based on their experimentally determined elution volumes, Stokes radii were estimated using the best fit line for the SR constructs.

Table 1
Kalirin spectrin repeat (SR) proteins expressed

The boundaries of SRs 1, 2, 3, 4, 5, 7 and 9 were identified using SMART¹⁵; based on manual alignment, two additional putative SRs were identified (SR6 and SR8). Additional residues were added to the N- and C-termini of the proteins expressed to try to increase their solubility. The name of each protein indicates the first and last putative SR contained in it. The predicted molecular weight (M_w) and absorption coefficient at 280 nm (A_{280}) for a 1.0mg/ml solution are shown. Each SR fusion protein was well expressed, but several fusion proteins were largely insoluble (*shown in italics*) and were not further analyzed.

SR fragment	Amino acids	M_w	Absorption coefficient, A_{280}
SR1:3	149-519	42.58	1.029
<i>SR2:4</i>	<i>282-632</i>	<i>40.43</i>	<i>insoluble</i>
<i>SR3:6</i>	<i>400-870</i>	<i>54.45</i>	<i>insoluble</i>
<i>SR3:7</i>	<i>400-976</i>	<i>66.57</i>	<i>insoluble</i>
<i>SR4</i>	<i>517-622</i>	<i>12.26</i>	<i>insoluble</i>
SR4:5	517-752	27.16	0.722
<i>SR5</i>	<i>624-752</i>	<i>14.91</i>	<i>insoluble</i>
SR5:6	622-870	28.96	0.677
SR4:6	517-873	41.21	0.684
SR4:7	517-976	53.39	0.765
SR7:9	869-1212	39.19	1.270
<i>SR8:9</i>	<i>966-1219</i>	<i>29.72</i>	<i>insoluble</i>
SR5:9	622-1208	68.14	1.108
SR9	1094-1257	19.38	1.106

Evaluation of SR structure using far UV circular dichroism

Far UV CD spectra were obtained for each SR protein. The calculated percentage of the structure accounted for by α -helix is shown, as is the $\Theta_{222\text{nm}}/\Theta_{208\text{nm}}$ ratio. Each protein was subjected to thermal denaturation as indicated in Methods; T_m values represent the average of at least two separate determinations.

Table 2

SR fragment	% α -helix	$\Theta_{222\text{nm}}$	$\Theta_{222\text{nm}}/\Theta_{208\text{nm}}$	T_m ($^{\circ}\text{C}$)	
				I	II
SR1:3	58	-21526	1.051	41±1.2	64±0.8
SR4:5	58	-23489	1.031	32±1.8	
SR5:6	45	-28564	1.065	42±1.1	
SR4:6	45	-35815	1.090	42±0.3	
SR4:7	47	-25610	1.046	31±0.5	46±1.7
SR7:9	49	-27513	1.058	46±0.9	
SR5:9	42	-23453	1.081	42±1.0	62±2.1
SR9	75	-15380	0.95	33±0.9	

Table 3
Guanidine and urea induced unfolding of SR proteins

Data from experiments like those shown in **Fig. 5** were used to calculate the concentrations of guanidinium HCl and urea producing a half-maximal effect on the structure of each SR protein.

SR Protein	Gdn.HCl _{1/2} [M]		Urea _{1/2} [M]	
	I	II	I	II
SR4:5	1.66	NA	2.03	NA
SR5:6	1.17	3.37	2.88	NA
SR4:6	1.67	3.36	2.29	5.6
SR4:7	1.67	3.42	2.81	5.48

Evaluation of hydrodynamic properties of Kalirin

A. Sedimentation velocity analysis of Kalirin proteins. Data from analyses like those shown in Fig.8 are summarized. The Stokes radius, R_S , was determined experimentally. R_{min} , the radius of a spherical protein, was calculated from M_w ($R_{min} = 0.066M^{1/3}$). The frictional ratio, f/f_{min} , ($= R_S/R_{min}$) gives an indication of asymmetry.

Table 4

SR Protein	M_w (fitted)	Ratio to predicted M_w	$S(20,w)$	R_s (nm)	f/f_{min}
SR1:3	40,700	0.956	2.76	3.69	1.60
SR4:5	28,400	0.956	2.35	2.76	1.37
SR5:6	30,600	1.057	2.32	2.98	1.45
SR4:6	40,700	0.988	2.90	3.40	1.47
SR4:7	52,100	0.976	3.06	4.14	1.65
SR7:9	42,500	1.084	2.77	3.32	1.46

B. Gel filtration analysis of Kalirin proteins. The proteins analyzed by analytical ultracentrifugation were used to calibrate a Superose 6 column. Recombinant SR5:9, Δ Kal7 and Kal7 were analyzed on the same column and a Stokes radius was assigned based on this calibration curve. Using R_s and R_{min} calculated for a monomer, a frictional ratio was determined.

SR Protein	M_w (based on sequence)	R_s (nm)	f/f_{min}
SR5:9	68,140	4.75	1.75
HisMyc Δ Kal7	119,784	5.47	1.71
HisMycKal7	191,349	6.13	1.63